OXYGEN ISOTOPIC COMPOSITION OF CA-FE-RICH SILICATES IN AND AROUND AN ALLENDE CA-AL-RICH INCLUSION. M. Cosarinsky[1], L.A. Leshin[1,2], G.J. MacPherson[3], A.N. Krot[4], and Y. Guan[1]. [1]Dept. of Geological Sci., Arizona St. Univ., Tempe, AZ, 85287-1404, [2]Center for Meteorites Studies, ASU; [3]Dept. of Mineral Sci., NMNH, Smithsonian Inst., Washington DC, 20560-0119; [4]Hawaii Inst. of Geophysics and Planetology, Univ. of Hawaii, Honolulu, HI, 96822. (cosarinsky@asu.edu)

Introduction: Most components of CV chondrites show variable degrees of late-stage alteration resulting in the modification of preexisting mineral assemblages and/or in the formation of new minerals. The conditions and environment under which these processes occurred are highly debated, with arguments in favor of solar nebular as well as asteroidal settings [1]. In the particular case of calcium-aluminum-rich inclusions (CAIs) these processes are typically evidenced by an Fe-alkali-halogen metasomatism, resulting in the formation of anorthite, nepheline, sodalite, grossular, wollastonite, diopside-hedenbergite-series pyroxene, andradite, and kirschsteinite. Similar mineral assemblages are also found in the matrices of these chondrites and in and around Allende dark inclusions. Detailed analysis and comparison of these late stage alteration phases in two different petrographic settings might offer better constraints on the formation conditions and environment. Therefore, we studied and compared the texture, mineralogy and chemical and oxygen isotopic composition of Ca-Fe-rich assemblages both in CAIs and the matrix of Allende, a member of the oxidized CV group in which these assemblages are very abundant.

Petrography: Allende TS24F1 is a large fluffy type A CAI [2] surrounded by an accretionary rim (AR) [3,4]. High-resolution X-Ray-area mapping highlights the distribution of Ca-Fe-rich silicates throughout the thin section (Fig. 1). The phases occur lining the exterior of Wark-Lovering rims (WLR), mostly filling internal cavities within the irregularly shaped CAI and in areas where the CAI is fractured, but they are also concentrated along the outer boundary of the accretionary rim (AR) where it contacts the matrix. The Ca-Fe-rich minerals also occur uniformly throughout the matrix [5]. Petrographically, the assemblages in contact with the CAI consist of relatively large (~20 μm) euhedral grains of andradite (*And*), hedenbergite (*Hed*), and massive to acicular wollastonite (*Wo*) and intermediate Ca-rich pyroxene (*Ca-px*). Directly contacting the WLR and the CAI itself, there are assemblages of *And* and *Hed* ($Fs_{>45}Wo_{\sim 50}$) intergrown with *Ca-px* ($Fs_{0\text{-}20}Wo_{\sim 50}$; Al_2O_3<15%), either as inclusions or as rims around them (Fig. 2). The FeO and Al_2O_3 contents of the *Ca-px* from this setting are highly variable over a micron-scale. Acicular fine-grained *Ca-px* ($Fs_{10\text{-}35}Wo_{\sim 50}$; Al_2O_3<5%) occurs as highly porous masses around the most FeO-rich minerals, in many cases with interstitial nepheline. *Wo* ($En_{<6}Fs_{<3}Wo_{>95}$) can occur as needles intergrown with *Hed* (Fig. 2b) or *Ca-px* as well as massive *Wo* inside euhedral *Hed* grains. Relict nodules of forsteritic olivine with sulfide cores occur within some of the *Hed* and *Ca-px* assemblages. The entire assemblages are surrounded by fine-grained fayalitic olivine.

The matrix occurrences are smaller (20-50 μm) and consist of texturally complex porous aggregates of intergrown *And* and pyroxene. They frequently have a zoned structure, with a core of *And* and/or *Hed* ($Fs_{>45}Wo_{\sim 50}$) surrounded by *Ca-px* ($Fs_{10\text{-}35}Wo_{\sim 50}$; Al_2O_3 < 2 %). Micron-sized *Ca-px* inclusions also occur within the cores. Loosely packed *Ca-px* grains mixed with fayalitic olivine laths usually mantle the entire assemblages (Fig. 3). *Wo* is usually absent or rare in these aggregates.

Isotopic Results: Oxygen isotopic analyses were acquired with the Cameca IMS 6f ion microprobe at ASU. Analyzed spots are about 15x10 μm and correspond either to individual mineral phases or mixtures of several grains. To correct for matrix effects, we repeatedly analyzed standards of olivine, andradite, and hedenbergite that are chemically similar to the target phases. Analyses of *Ca-px* and *Wo* were corrected with the hedenbergite standard. Most of the data plot along a mass-dependent fractionation trend slightly below the terrestrial fractionation line (TFL) ($\Delta^{17}O \sim -3$ ‰; $2\sigma \sim \pm 3$ ‰), coincident with the so-called Allende mass fractionation line [6,7]. Overall, the data plot to the right of the CAI line with a ~ 20 ‰ spread in $\delta^{18}O$ values (Fig. 4). A few points plot at more ^{16}O-rich values close to the CAI line ($\Delta^{17}O = -6$ to -11 ‰). Mineralogically, these ^{16}O-rich data points correspond to *Ca-px* (Al_2O_3 ~ 10-15 %) and *Hed* that are probably mixed with ^{16}O-rich relict phases (*e.g.*, spinel, fassaite, olivine). There is no strong mineralogical control on the isotopic composition of all phases analyzed, although the spread in *Wo* is shifted by ~5 ‰ towards lighter compositions compared to the rest of the data. Data ranges of phases from the matrix overlap those data of phases from within the CAI, although matrix phases tend to plot on the heavier end of the trend.

Discussion: In this study, we find textural, chemical, and isotopic similarities among the assemblages that occur in contact with the CAI, along the AR-matrix boundary and in the matrix. Thus, it is likely that all phases share a similar origin. MacPherson and Krot [5] compared the occurrence of Ca-Fe-rich silicates between reduced and oxidized CVs and concluded that, even though they are more common in the oxidized subgroup, their occurrence is controlled by the porosity of the host rock, therefore implying a parent body control on their formation. According to this, it is reasonable to conclude that these assemblages formed by the interaction of the accreted components (CAI, AR, and matrix) with parent body fluids that percolated through pore spaces and precipitated most of the assemblages in open cavities within the CAI and in fractured areas, as well as along a major textural boundary like that between the AR and matrix. The chemical composition of such fluid may have been attained by reaction with Ca-rich primary minerals from the CAI and Fe,Ni-metal. Comparable Ca-Fe-rich assemblages in and around Allende dark inclusions [8], magnetite and fayalite from oxidized CVs [9,10], and Vigarano Mg-kirschsteinites [11] are also similarly depleted in ^{16}O as the phases in this study, suggesting that they all formed by interaction with an isotopically heavy, ^{16}O-depleted reservoir. Given the textural, mineralogical, chemical and isotopic similarities between the Ca-Fe-rich assemblages associated with dark inclusions and those with CAIs, it is likely that they all formed *in situ* dur-

ing alteration of the Allende parent body, as proposed for the dark inclusion assemblages [12,13].

References: [1] Krot A.N. et al. (1995) *Meteoritics, 30*, 748-775. [2] MacPherson G.J. and Grossman L. (1984) *GCA, 48*, 29-46. [3] MacPherson G.J. et al. (1985) *GCA, 49*, 2267-2279. [4] Cosarinsky M. et al. (2002) *Meteoritics & Planet. Sci., 37,* A38. [5] MacPherson G.J. and Krot A.N. (2002) *Meteoritics & Planet. Sci, 37,* A91. [6] Ash R.D. et al. (1999) *LPS XXX*, Abstract #1836. [7] Young E.D. et al. (1999) *Science, 286*, 1331. [8] Krot et al. (2000) *LPS XXXI*, Abstract #1463. [9] Choi B.G.et al. (1997) *EPSL, 146*, 337. [10] Choi B.G. et al. (2000) *Meteoritics & Planet. Sci., 35,* 1239. [11] Cosarinsky et al. (2001) *LPS XXXII*, Abstract #1859. [12] Krot A.N. et al. (1998) *Meteoritics & Planet. Sci., 33,* 623. [13] Krot A.N. et al. (2000) *Geochem. International, 38* Suplement S351.

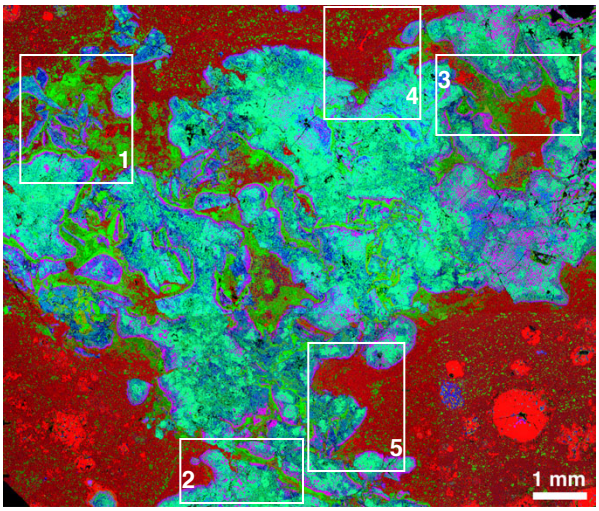

Fig. 1 Combined Mg (red), Ca (green) and Al (blue) XR elemental maps of Allende TS24F1 showing the distribution of Ca-Fe-rich (bright green) phases within the CAI (blue-purple-aqua) and concentrated along the AR-matrix boundary, and throughout the matrix. The red area corresponds to the Mg-rich AR, matrix and chondrules. The white boxes indicate the areas considered in this study.

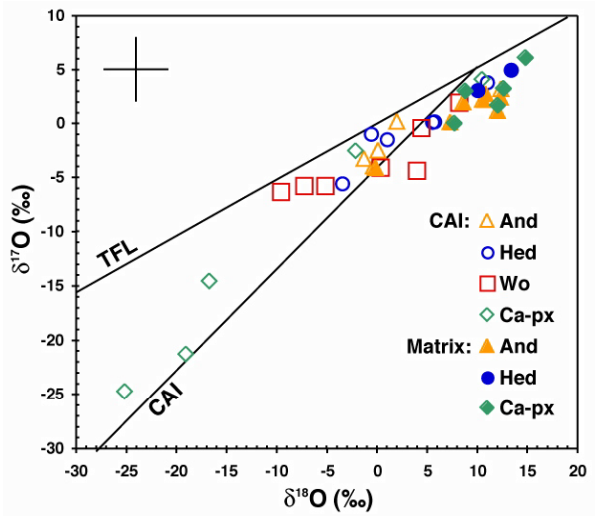

Fig. 4 Oxygen isotopic composition of *And*, *Hed*, *Ca-px*, and *Wo* that occur next to the CAI and within cavities in it (open symbols; areas 1, 2 and 3 in Fig. 1) and in the matrix (solid symbols; areas 4 and 5 in Fig. 1). Typical 2σ errors are ±3‰.

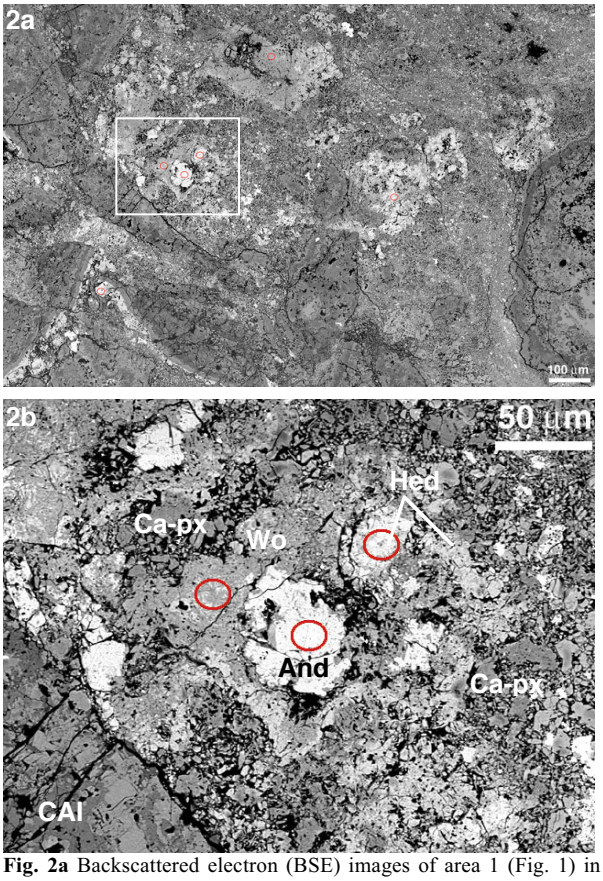

Fig. 2a Backscattered electron (BSE) images of area 1 (Fig. 1) in which Ca-Fe-rich silicates grow next to broken pieces of the CAI (upper left) and over its WLR (lower left), partially filling cavities within the CAI. **2b** Detailed images of *And*, *Wo* intergrown with *Hed*, and *Ca-px* from area highlighted in Fig. 2a. Red circles indicate the ion probe spots.

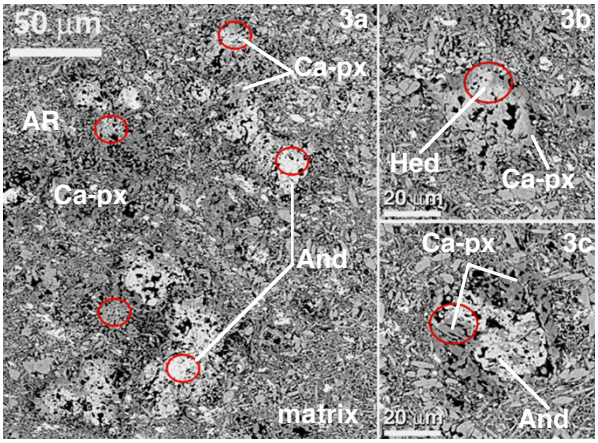

Fig. 3 Detailed BSE images of Ca-Fe-rich silicates concentrated along the AR-matrix boundary (area 5 on Fig. 1). **3a** Several aggregates comprised of a porous core of mostly *And* and a rim of *Ca-px*; the assemblages are surrounded by acicular *Ca-px* and lath-shaped fayalitic olivine from the AR and matrix. **3b** Small aggregate of *Hed* (core) and *Ca-px* (rim). **3c** Porous *And* with small *Ca-px* inclusions and a *Ca-px* rim around it. Red spots indicate the areas analyzed with the ion probe.